AN INVESTIGATION ON THE VARIATION OF THE PRESSURE DISTRIBUTION FOR COMPRESSIBLE LAMINAR FLOW IN A CHOKED-FLOW TUBE DUE TO CHANGES OF THE BACK PRESSURE

by

Jorge A. Lazo Gallo

Submitted in Partial Fulfillment
of the Requirements for the
Degree of Bachelor of Science
at the
MASSACHUSETTS INSTITUTE OF TECHNOLOGY

June, 1961

Signature of Author . Signature redacted
Department of Mechanical Eng., June, 1961

Certified by . . Signature redacted .
Thesis Supervisor

Accepted by . . . . . Signature redacted
Chairman, Departmental Committee on Theses

ACKNOWLEDGMENTS

The author is grateful to all those who willingly helped in preparing this thesis.

The author would like to express his appreciation to Professor Alve Erickson, who, as supervisor of this thesis gave freely of his time and encouragement.

The author is indebted to Professor G. A. Brown for the use of the facilities which made this experimental work possible.

AN INVESTIGATION ON THE VARIATION OF THE PRESSURE DISTRIBUTION FOR COMPRESSIBLE LAMINAR FLOW IN A CHOKED-FLOW TUBE DUE TO CHANGES OF THE BACK PRESSURE

by

Jorge A. Lazo

Submitted in Partial Fulfillment
of the Requirements for the
Degree of Bachelor of Science
at the
MASSACHUSETTS INSTITUTE OF TECHNOLOGY
June, 1961

ABSTRACT

An experimental investigation has been carried out to determine if there is any noticeable effect on the static pressure distribution in a choked-flow tube when the exhaust stagnation pressure is changed. A laminar flow of air in a constant area tube and a boundary layer thickness of about half the radius were used to perform the experimental part of this investigation. The results indicate that the boundary layer thickness may go through a maxima at a region where M = 1 and thin down to account for the exit Mach Number of 1.23, 1.21 and 1.06 that were obtained through the assumption of an isentropic-core flow.

Thesis Supervisor: Alve J. Erickson

Title: Assistant Professor of
Mechanical Engineering

TABLE OF CONTENTS

NOMENCLATURE

D = Flow-tube diameter

H = Thwaites' Function

L = Flow-tube Length

M = Mach Number

P = Pressure

P* = Pressure at M = 1

R = Flow-tube Radius

T = Temperature

V = Velocity

m = Thwaites' Function

x = Length measured along flow-tube

δ = Boundary layer thickness

δ^* = Boundary layer displacement thickness

ν = Kinematic viscosity

θ = Momentum thickness

Subscripts

b - Downstream stagnation properties

e - Exxt plane properties

o - Upstream stagnation properties

I - INTRODUCTION

It has been accepted that an infinitesimal pressure pulse originating downstream of a region where the local fluid speed is higher or at least equal to that of sound, will not travel upstream across it. The speed of the pressure pulse is a relative speed with respect to the medium in which it travels; if the medium itself is moving in any given direction with a velocity equal to that of sound it would seem, to an observer at rest, that the pressure pulse is stationary; that is, it does not propagate upstream in the moving fluid.

In the absence of friction, there would be no forces trying to retard the fluid moving close to the walls and therefore the velocity of the fluid, at any cross-section, would be uniform. However, because of viscocity the fluid next to the wall is brought to rest; this sets up a velocity profile that grows from zero at the wall interface to the free stream core velocity at its edge, the shape of this velocity profile can be approximated by a parabola.

Since the velocities in the boundary layer are considerably smaller than those in the main stream, there is the possibility of the infinitesimal pressure pulse propagating upstream through this boundary layer even when the free stream core velocity is supersonic. This assumes the existence of a boundary layer at all times, which is a valid assumption if we confine ourselves to "real" fluids.

It is the aim of this thesis to investigate this latter effect

and determine whether the strength of the pressure pulse, progressing upstream through the boundary layer, is enough to alter the conditions upstream when a sonic or super-sonic region exists in the duct.

II - APPARATUS DESIGN

The nozzle block has been designed to produce a laminar compressible flow in the tube; provision has been made to measure the static pressure along the length of the tube axis close to the exit plane of the block.

In a paper by Rivas and Shapiro, it was found that the maximum length Reynolds number (Re_x) for the existence of a laminar boundary layer in a stream with moderate initial turbulence, is about $5x(10)^5$, from this, the range of diameter Reynolds number (Re_d) in which laminar flow can be expected is determined by,

$$Re_d = \rho VD/\mu = (\rho Vl/\mu)(D/L) = Re_x(D/L) = 5 \times 10^5 \times (D/L)$$

For design purposes, a maximum diameter Reynolds number of $(10)^4$ was chosen. Air at room temperature was selected as the working fluid. To facilitate the basic design calculations, it was assumed that the behaviour of the boundary layer in the duct could be approximated by that of a flat plate. This assumption, as verified in a paper by Toong and Shapiro, is valid if the ratio of the boundary layer thickness to the tube radius is kept small. In this instance, therefore, we can use the familiar relation obtained by Blasius that related the thickness of the boundary layer to the flow length, i.e. $\delta = 5.2\ x\ /\ Re_x$; the tube length necessary to produce a boundary layer of about one-third the radius can be calculated. After consideration of these criteria and the available laboratory apparatus, the following physical dimensions and fluid conditions were chosen:

Air

T_o = room temperature = 85^o F.

P_o' = 2 psia. or less

Tube Dimensions

D = tube diameter = .200 inches

L = tube length = 3 1/16 inches

The air stream is led into the tube by a converging nozzle which conforms to the ASME specifications for a long-radius flow nozzle. A more detailed description of the flow tube and nozzle will be found in figure 1.

A travelling pressure probe was used to measure the static pressure along the axis of the flow tube. This method was originally suggested by Professor Ascher H. Shapiro and has the advantage, over the standard pressure taps, that errors due to blurs in the pressure taps would be the same for all readings and that measurements could be made at any desired location along the tube length.

The static pressure probe was constructed from a seven inch length of hypodermic needle tubing of .016 inches outside diameter and a .004 inches wall thickness. Two holes of .007 inches diameter were made in the wall of the tubing. The presence of the pressure probe in the flow tube will have some effect on the flow pattern and flow rate, but since the probe area represents only 0.64% of the flow tube area, we assume that this effect is negligible.

The following is a description of the apparatus in general and can be best followed by referring to Figure 2. In the picture we can see what will be referred to as the test box, which is a steel box with outside dimensions of about 12 x 10 x 18 inches. The flow tube and the travelling pressure probe mechanisms are enclosed in this box because the system is designed to operate at pressures much lower than atmospheric pressure.

The flow tube is attached to the wall that divides the test box into upstream and downstream stagnation areas. The flow into and through the test box is from right to left. Air from the atmosphere is admitted, through a pipe and control valve at the right, to the upstream stagnation area. The air flows through the nozzle and tube, and exhaust through an opening, in the divider wall, into the downstream stagnation area. The flow then leaves the test box through a two inch pipe which in turn is connected to a three-stage ejector through another control valve.

The two micrometer heads, one at either end of the testbox, hold the static pressure probe and allow it to pass completely through the flow tube. These micrometer heads position the probe at any desired location along the axial direction of the flow tube; the total distance that the probe can travel is about one inch. The micrometer head at the bottom of the test box is attached directly to the tube and nozzle block, this allows a precise location of the flow tube in the vertical plane. Hence the pressure probe is free to move in the axial direction to any position we want and can be adjusted to take measurements along a diameter of the flow tube.

All the leads that connect the pressure probe, downstream and upstream stagnation pressure taps to the manometer board, pass through vacuum seal in the wall of the test box. The reference pressure for the whole system is the amount of vacuum that can be obtained from a vacuum pump and this in turn is measured with a McLeod gauge. The gauge is shown to the right of the test box. The stagnation temperature of the flow is measured with a thermometer which passes through the top of the test box into the upstream stagnation area.

The vacuum diffusion pump oil used in the manometers was Narcoil 40, its low vapor pressure and viscocity make it suitable to use in manometers. Tables of pressure conversion factors for the manometer fluid and mercury, which is used in the McLeod gauge, are given in the appendix.

III EXPERIMENTAL RESULTS

A Experimental Procedure

All the data which is presented here was obtained entirely from pressure readings on the manometer board. Initial test runs showed a continuous drift of the back pressure provided by the ejector, this variation of back pressure was not, in any run, big enough to be taken into account in the calculations. The pressure probe was found to be very reliable and at no time gave much trouble, although it does have some serious limitations. The time response of the probe to changes of pressure is slow due to the combination of a 2 inch length and a .008 inch diameter flow section (see figure 3); it was experimentally determined that it took the pressure probe about 45 minutes to give reliabele readings, for every pressure measurement taken. The total travel of the probe along the axis of the flow tube is limited to one inch and although this did not hinder our experiment, it might be a serious limit in other experiments where readings over a length of more than one inch are to be taken.

An experimental run consisted of setting the stagnation and back pressure at a desired level, setting the probe at a determined place, and after 45 minutes move it to the next station, and so on, until all readings for that particular run were taken. Seven readings were taken for each run, at 0.100 inch intervals starting at the exit plane. The total length of the flow tube covered in this way was 0.600 inches or three times the flow diameter. It took about 5 hours to complete the readings for any one of the runs. After every run the back pressure was set to a

new level without varying the upstream stagnation pressure, and another set of pressure measurements taken.

Figures 4, 5, and 6 show graphs of the data that was obtained. Figure 5 is an amplification of runs 6, 7, and 1 which do not show very well in figure 4. In both graphs the pressure along the duct has been normalized with the upstream stagnation pressure. Figure 6 shows the actual value of the static pressure as a function of the flow length, where the zero length corresponds to the exit plane of the flow tube.

B. Comparison of Experimental Data with a Choked-Constant-Area Flow in a Duct

Figure 7, is a plot of the values of P_e/P_o versus P_b/P_o. The corresponding ratios for all the experimental runs are included in this graph. Classical theory predicts that there would be no changes in the value of P_e/P_o until the critical value of this ratio is reached and the choked condition no longer exists; this results in a constant value of P_e/P_o (horizontal line in figure 7), until the unchoked condition requires that the ratios P_e/P_o and P_b/P_o be equal (45^o line). The plot of the data in figure 7 does show a small departure from classical theory. The line that should appear as a horizontal line is inclined at a small angle. In the following paragraphs it will be tried to find out just how much the flow departs from the predictions of classical theory for a choked-constant-area-flow.

C. The Theoretical Fanno Line and the Experimental Data

As a first attempt, it was tried to compare our data with the

theoretical Fanno Line. To do this, it was assumed that the exit Mach number for runs 6, 7, and 1 was equal to one and that therefore the pressure at the exit plane was equal to P*; the Fanno Line was then drawn through this point, as is shown in figure 8 by the solid line. The data from runs 6, 7, and 1 appear in this figure as points. The differences between the data and the Fanno Line are not big enough to justify a serious departure from this theory. Further calculations with the Fanno Line were made in the following way, making the length from entrance to exit of the flow tube equal to L_{max} a value of P/P* was found from the Fanno Line; from this and assuming isentropic flow through the entrance nozzle a theoretical value of P* was calculated and compared with the values obtained from the data. These results are tabulated below.

Runs	P*(data, psia)	P*(Fanno, psia)
1	.613	.645
6	.740	.776
7	.725	.760

These results imply that the behaviour of the flow in the duct does not follow the predictions of the Fanno Line, which means that the flow is not, solely, friction flow, and that further evaluation of the data is required to be able to find the answer sought.

The friction factor for the flow from Fanno Line considerations was found to be 0.01225 which seems to be a little high, but this is an apparent friction factor obtained only from pressure measurements.

D. Isentropic Core Flow

Assuming an Isentropic Core in the flow, the corresponding Mach Numbers were calculated and are presented in figure 9 as a plot of Mach Number vs. Length. This assumption is justified by the presence of the boundary layer. All transfer processes are confined to the boundary layer leaving, in the central axis of the duct, an isentropic core, this if the boundary layers that grow from opposite sides of the tube do not come in contact with each other (see figure 11).

Figure 9 shows a definite departure from theory of fully developed flow. In theory, if the flow at the entrance of the duct is subsonic, it could not go supersonic at any section of the tube and at most it would go sonic at the exit plane in what is known as choked flow.

Using the isentropic core flow assumption the exit plane Mach numbers were found to be 1.23, 1.21 and 1.06 for runs 1, 6 and 5 respectively, which as was said before, departs seriously from classical theory.

E. Thwaites' Method for Laminar Boundary Layer

A finer correlation between our experimental data and the theory of boundary layer growth was provided by comparing the results of boundary layer calculations using some experimental data with those obtained by using the method of Thwaites (see References). A brief outline of this method follows.

$$\delta^* = H\theta \tag{1}$$

$$\frac{d\delta^*}{d} = H + \theta \frac{dH}{d\theta} \tag{2}$$

$$H = H(m); \quad \text{where,} \quad m = -\frac{\theta^2}{\nu} \frac{dV}{dX} \tag{3}$$

$$\frac{dm}{d} = - \frac{2\theta}{\nu} \frac{dV}{dx} \tag{4}$$

$$\frac{d}{d}\frac{\delta^*}{\theta} = H + \theta \frac{dH}{dm} \frac{dm}{d\theta} = H - \frac{2\theta^2}{\nu} \frac{dV}{dx} \frac{dH}{dm} \tag{5}$$

if δ^* is to have a maximum:

$$\frac{d}{d}\frac{\delta^*}{\theta} = 0 = H - \frac{2\theta^2}{\nu} \frac{dV}{dx} \frac{dH}{dm} \tag{6}$$

$$\frac{dV}{dx} = \frac{H}{\frac{2\theta^2}{\nu} \frac{dH}{dm}} \tag{7}$$

Assuming a linear growth of the core velocity in the form

$$V = V_o \left(1 + a \frac{x}{L}\right) \tag{8}$$

therefore and after integration

$$\theta^2 = \frac{.45}{6} \frac{L}{a} \frac{\nu}{V_o} \left[1 - \frac{1}{\left(1 + a \frac{x}{L}\right)^6}\right] \tag{9}$$

from equation (3) and equations (8) and (9),

$$m = - \frac{\theta^2}{\nu} \frac{dV}{dx} = - \frac{\theta^2}{\nu} \frac{V_o}{L} = - \frac{.45}{6}\left[1 - \frac{1}{(1 + a)^6}\right] \tag{10}$$

and m can then be calculated and H and $\frac{dH}{dm}$ found from figure 10; this gives a numerical value of $\frac{dV}{dx}$ that would maximize δ^*. This value was compared to the value of

$$\frac{dV}{dx} = - \frac{dP/dx}{\rho V}$$

evaluated at M = 1. The results were:

Run	$\frac{dV}{dx}$ (Thwaites, $\frac{ft/sec}{ft}$)	$\frac{dV}{dx}$ (exp., $\frac{ft/sec}{ft}$)
7	2800	4300
1	2410	3410

Both results agree within less than an order of magnitude, which is a very good agreement if it is taken into account that the assumption of a linear increase of the core velocity is only a gross approximation.

F. Flat Plate Results

Figure 10 is a plot of the ratio δ/R for runs 1 and 6; run 4 was included in the plot to have something to compare with. To calculate the boundary layer thickness at each point, the following relationship was used:

$$\frac{\delta}{x} = \frac{5.2}{\sqrt{\frac{Vx}{\nu}}} \qquad \frac{\delta}{R} = \frac{5.2(x/R)}{\sqrt{\frac{Vx}{\nu}}}$$

This relation is valid in the case of no pressure gradient. If a pressure gradient exists, as in our case, the boundary layer would be thinner.

The results of these calculations show, as is clearly seen in figure 11, that the boundary layer displacement thickness may go through a maximum at M = 1, and thin down to form a kind of convergent-divergent nozzle for the core flow which would account for the supersonic speeds of the flow near the exit plane.

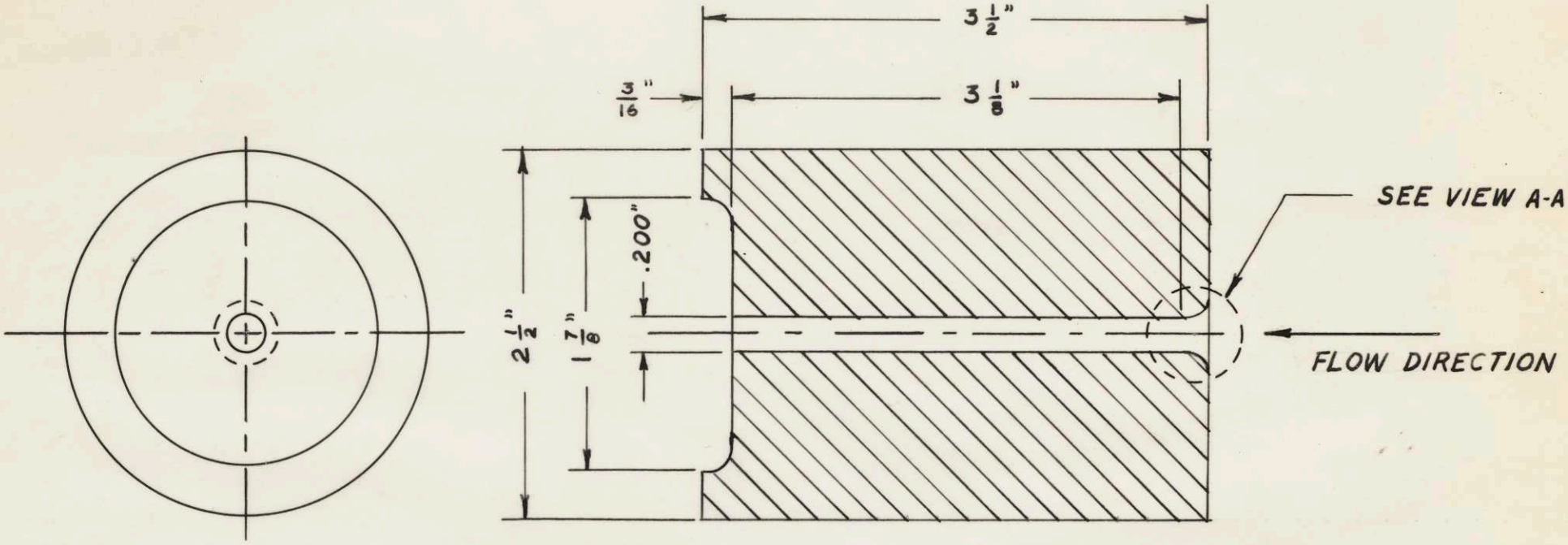

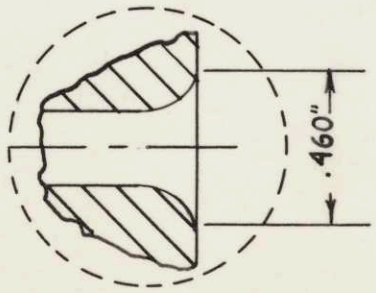

VIEW A-A

FIGURE 1

FLOW - DUCT

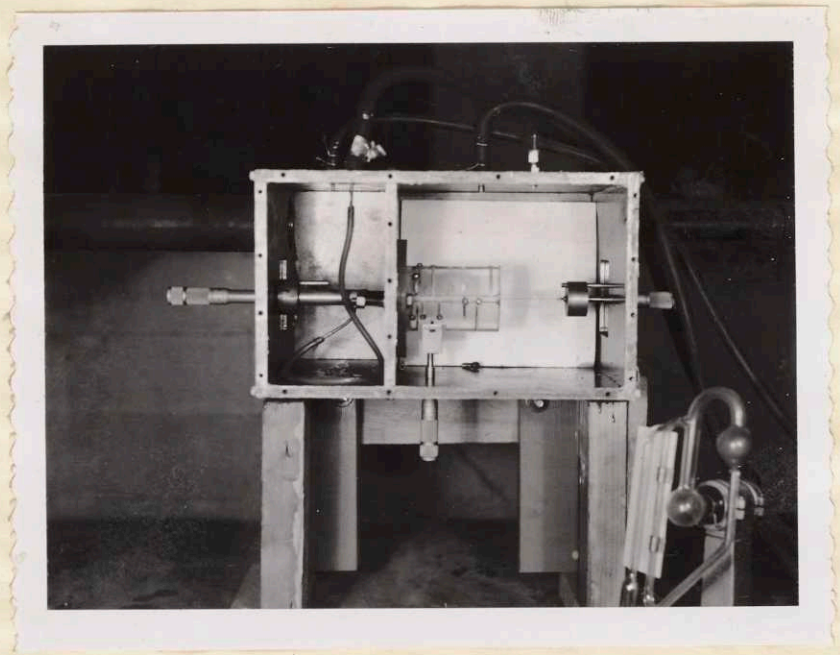

FIGURE 2

EXPERIMENTAL APPARATUS

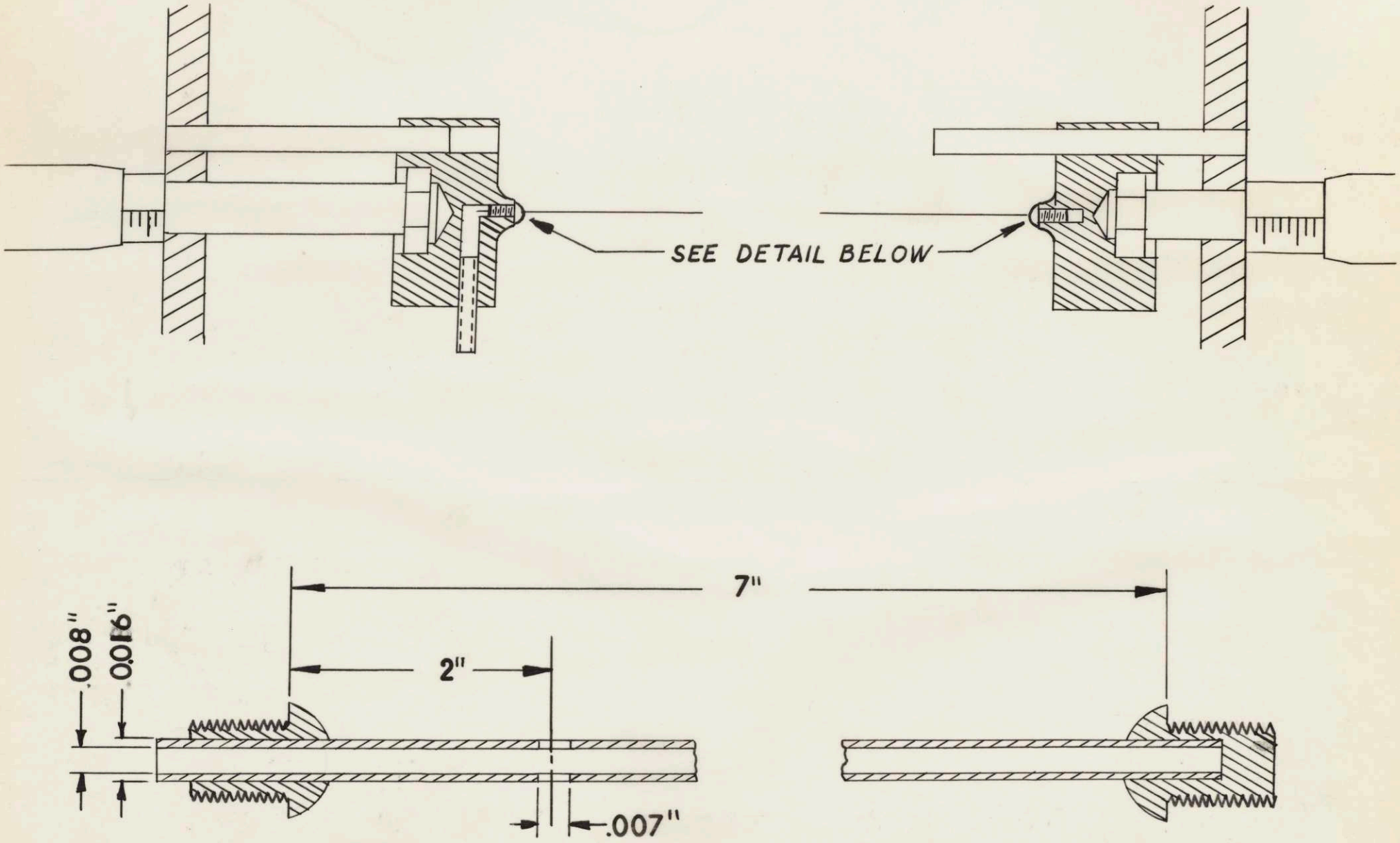

FIGURE 3

PRESSURE PROBE MECHANISM

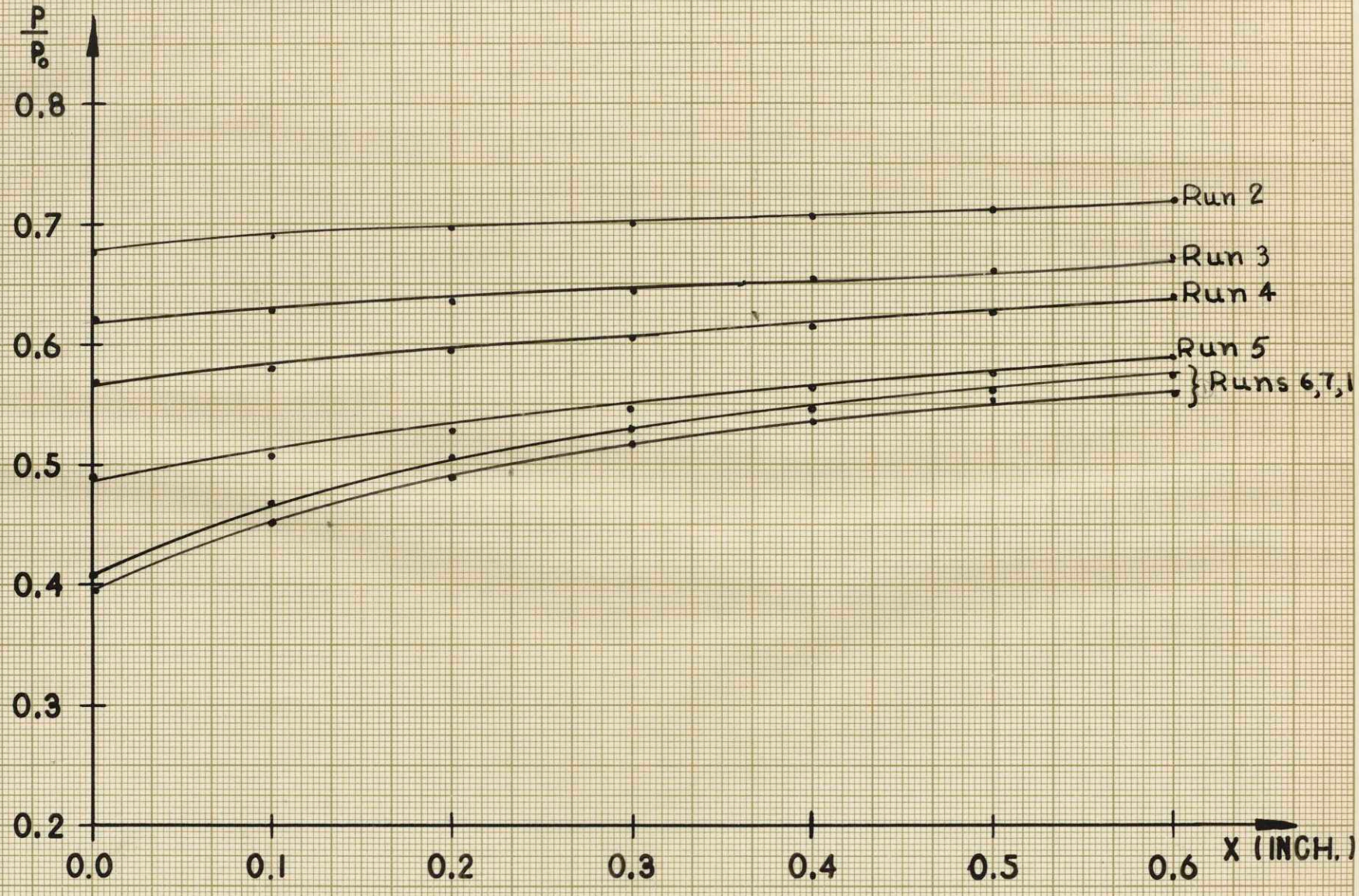

FIGURE 4

PRESSURE DISTRIBUTION ΔLONG Δ DUCT

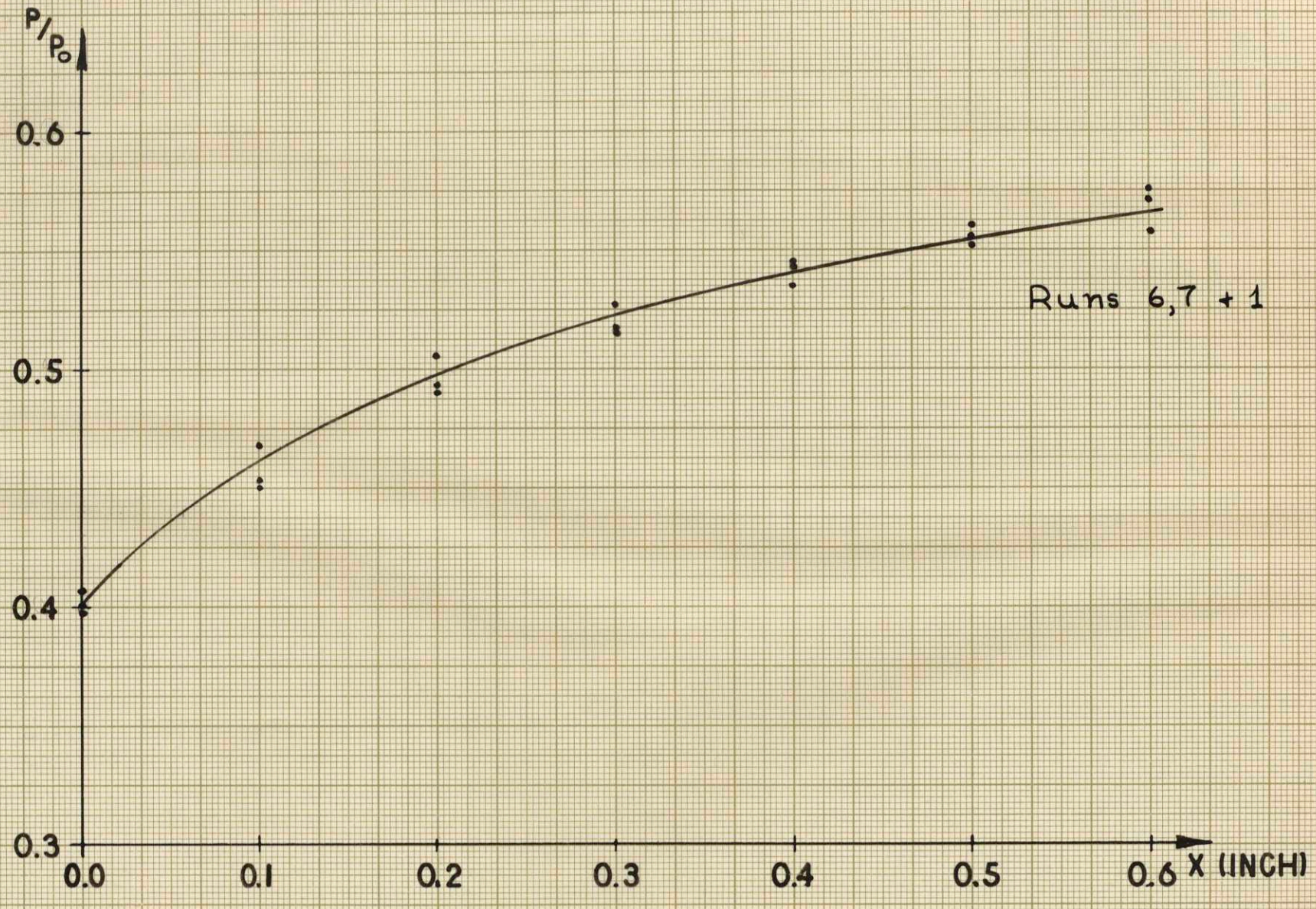

FIGURE 5

PRESSURE DISTRIBUTION ALONG THE DUCT

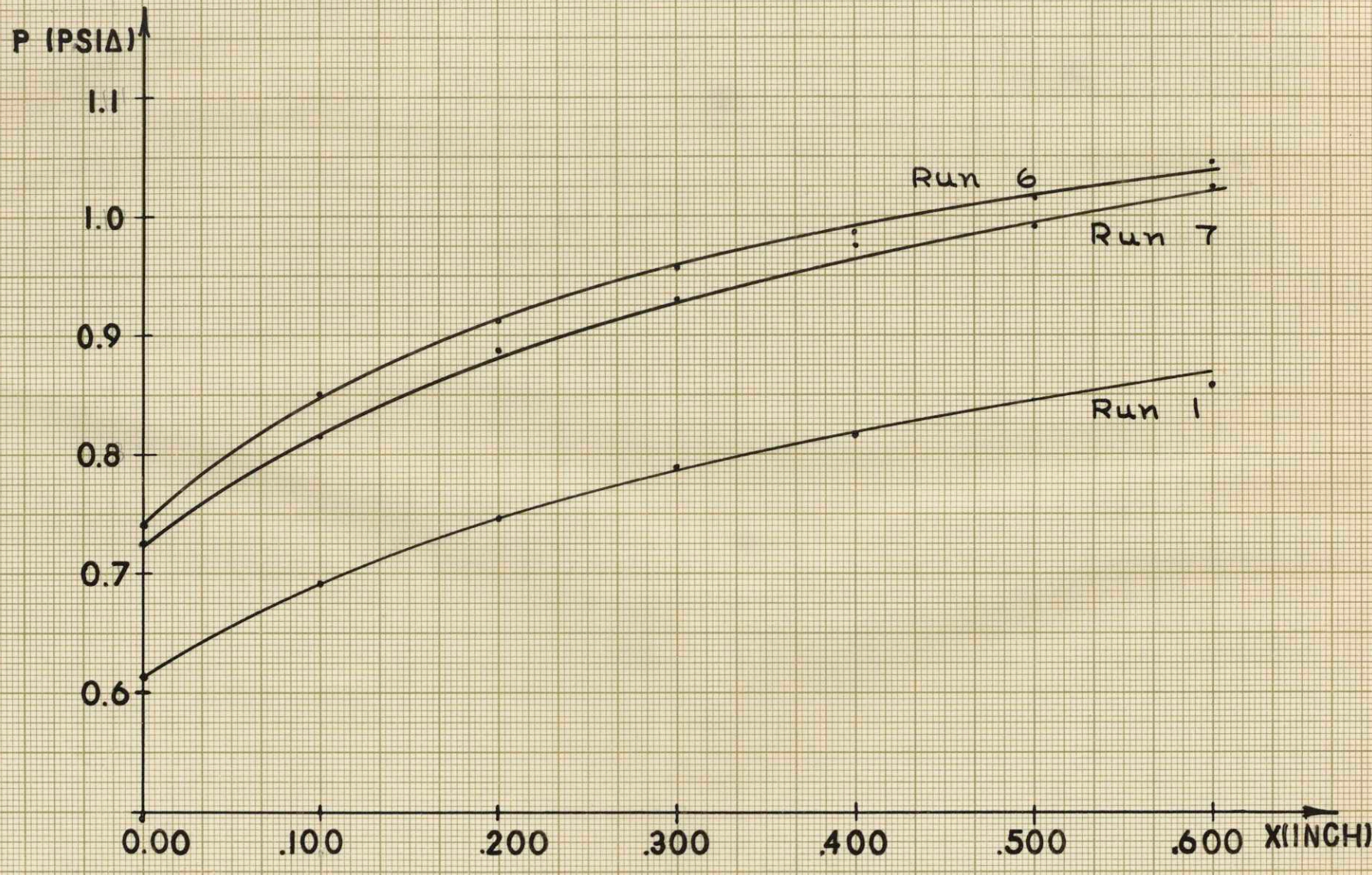

FIGURE 6
STATIC PRESSURE DISTRIBUTION

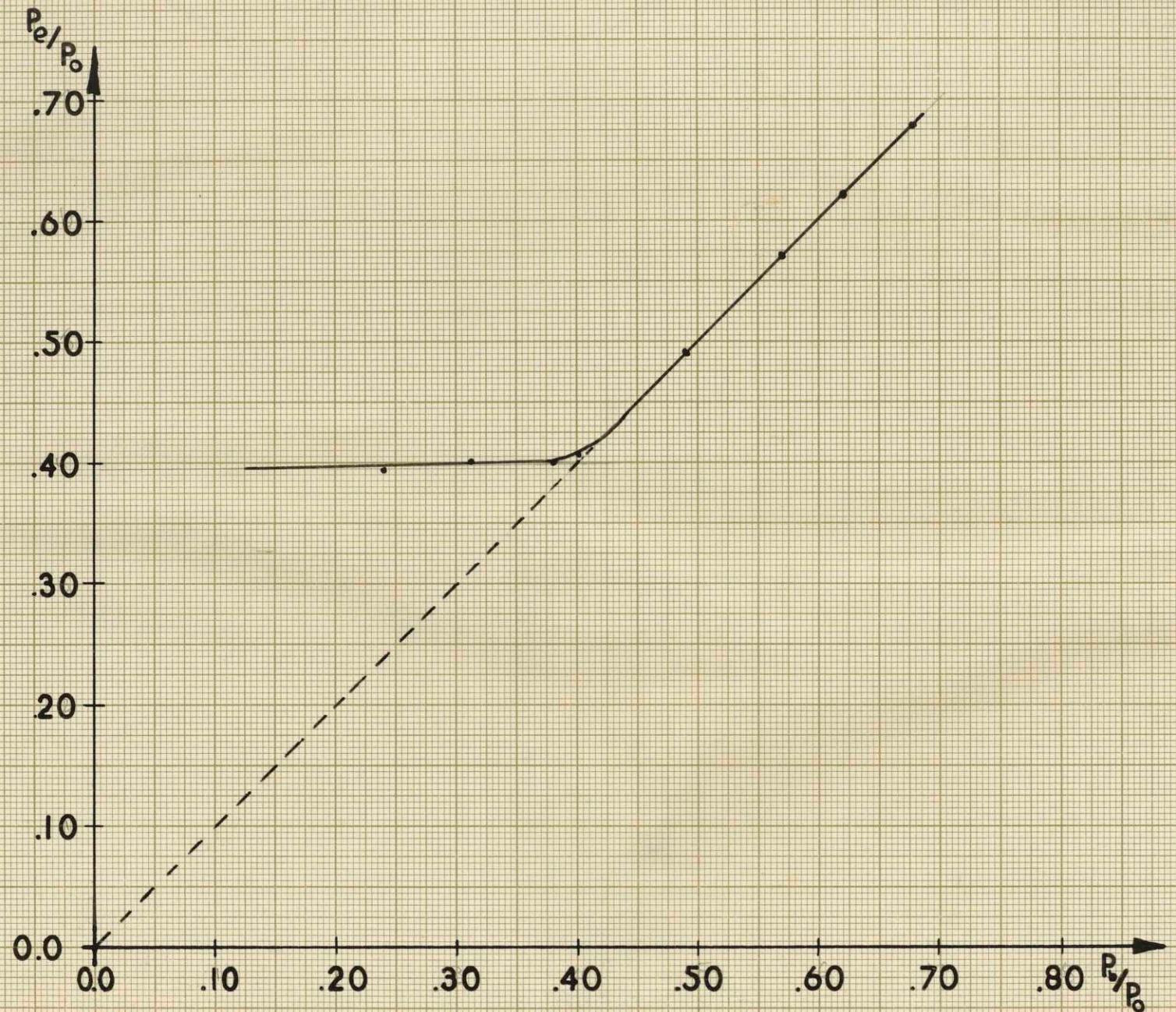

FIGURE 7

EXIT PLANE PRESSURE VS. BACK PRESSURE

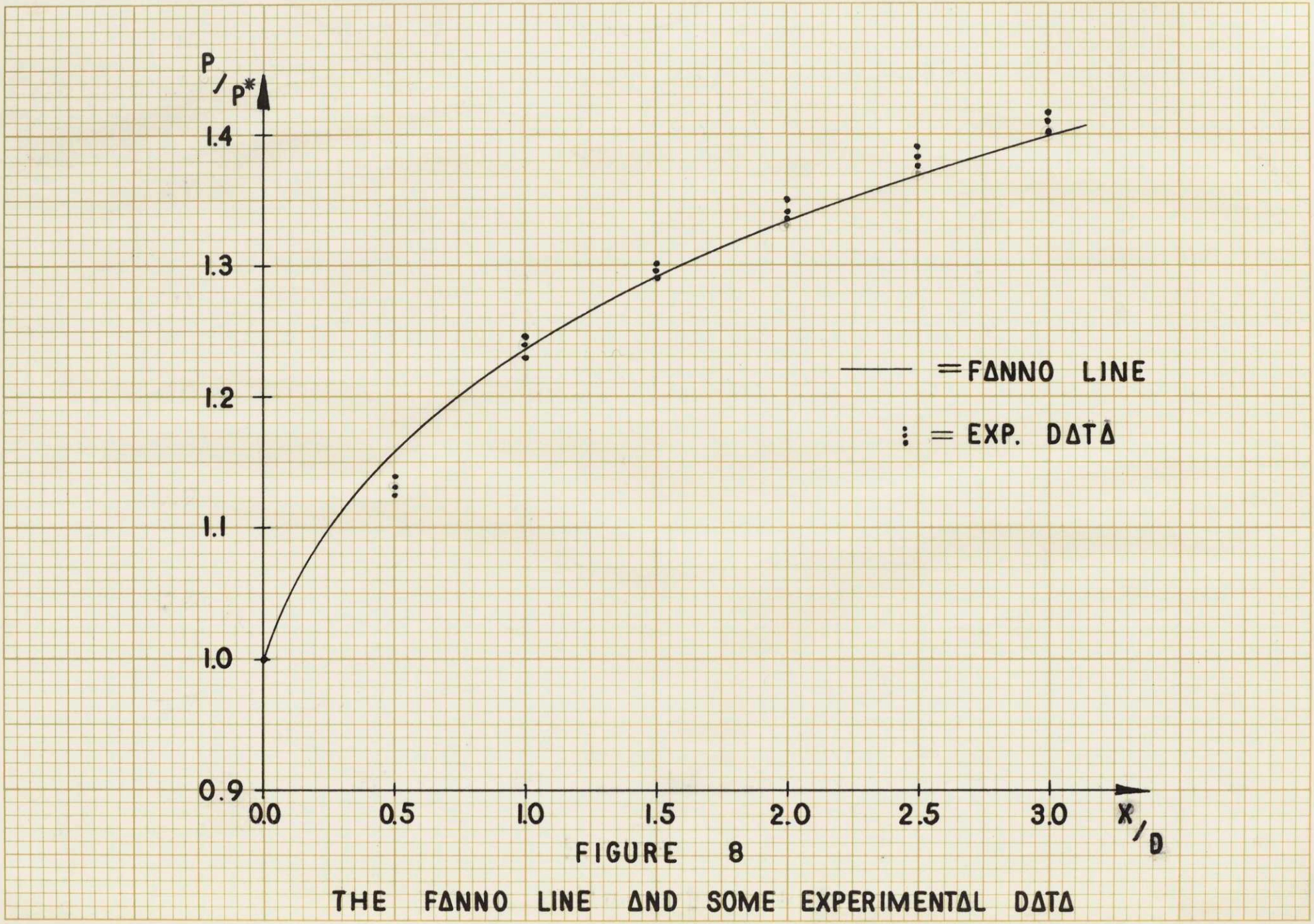

FIGURE 8

THE FANNO LINE AND SOME EXPERIMENTAL DATA

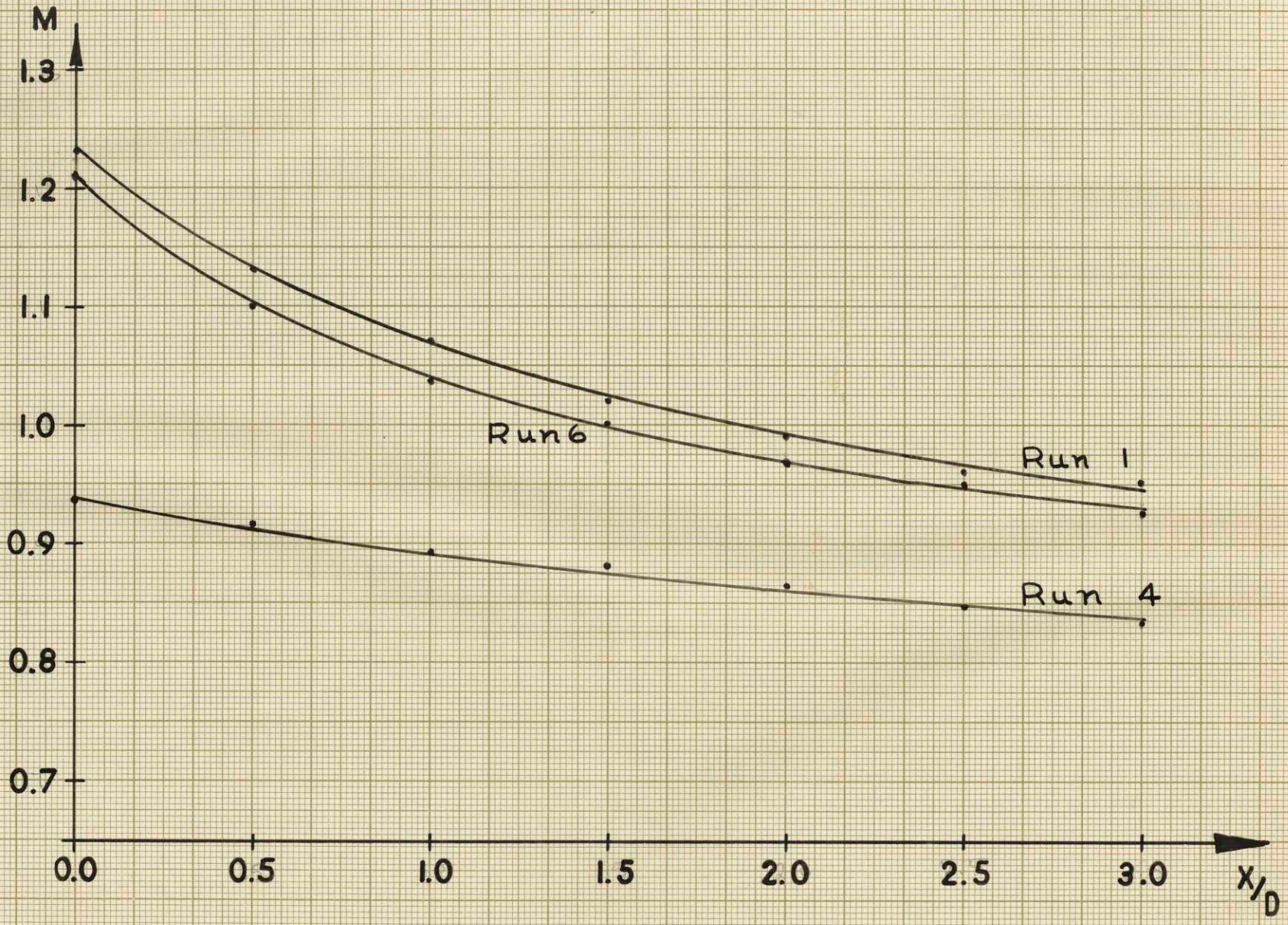

FIGURE 9

MACH NUMBER DISTRIBUTION

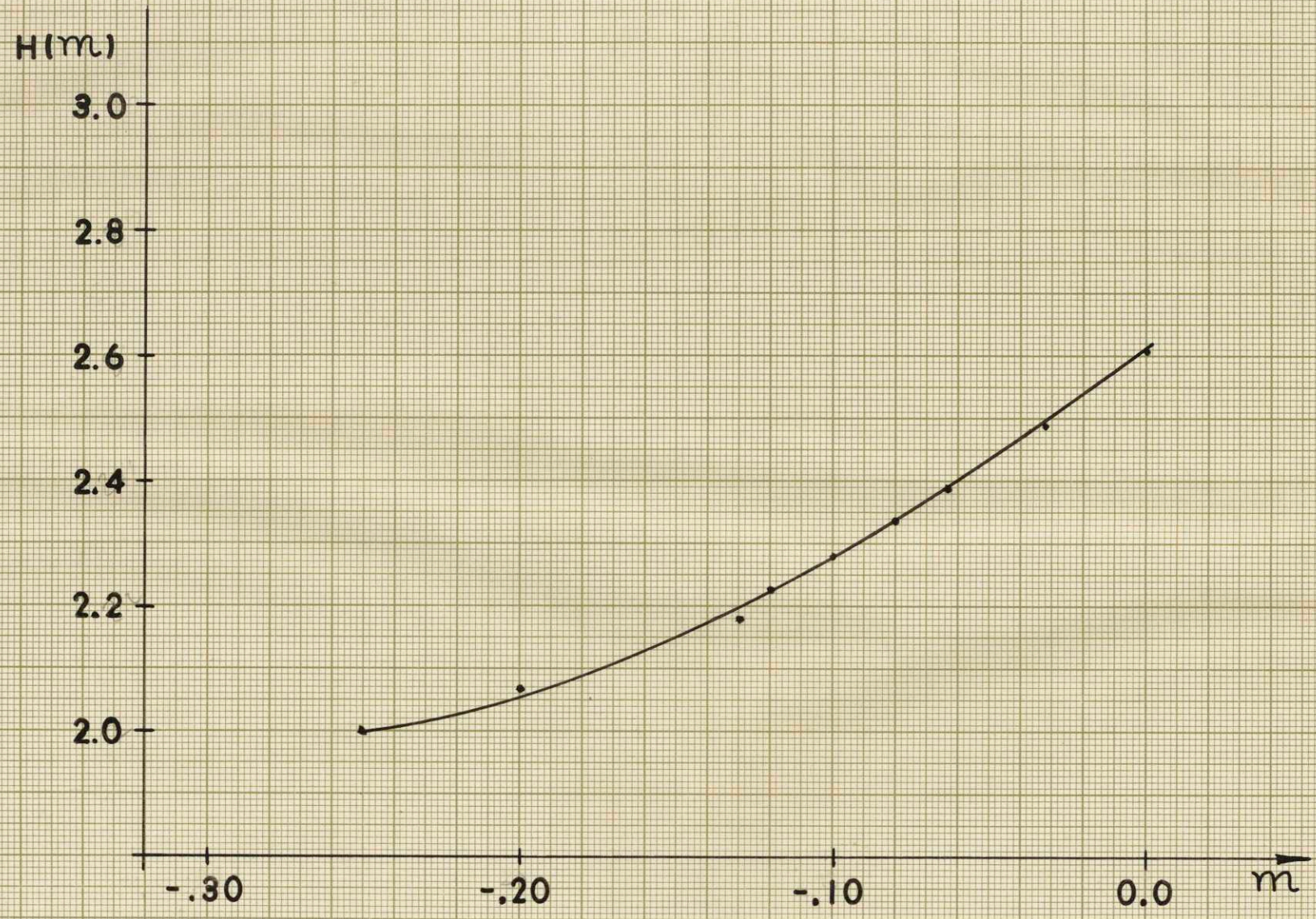

FIGURE 10

THWAITES' FUNCTIONS

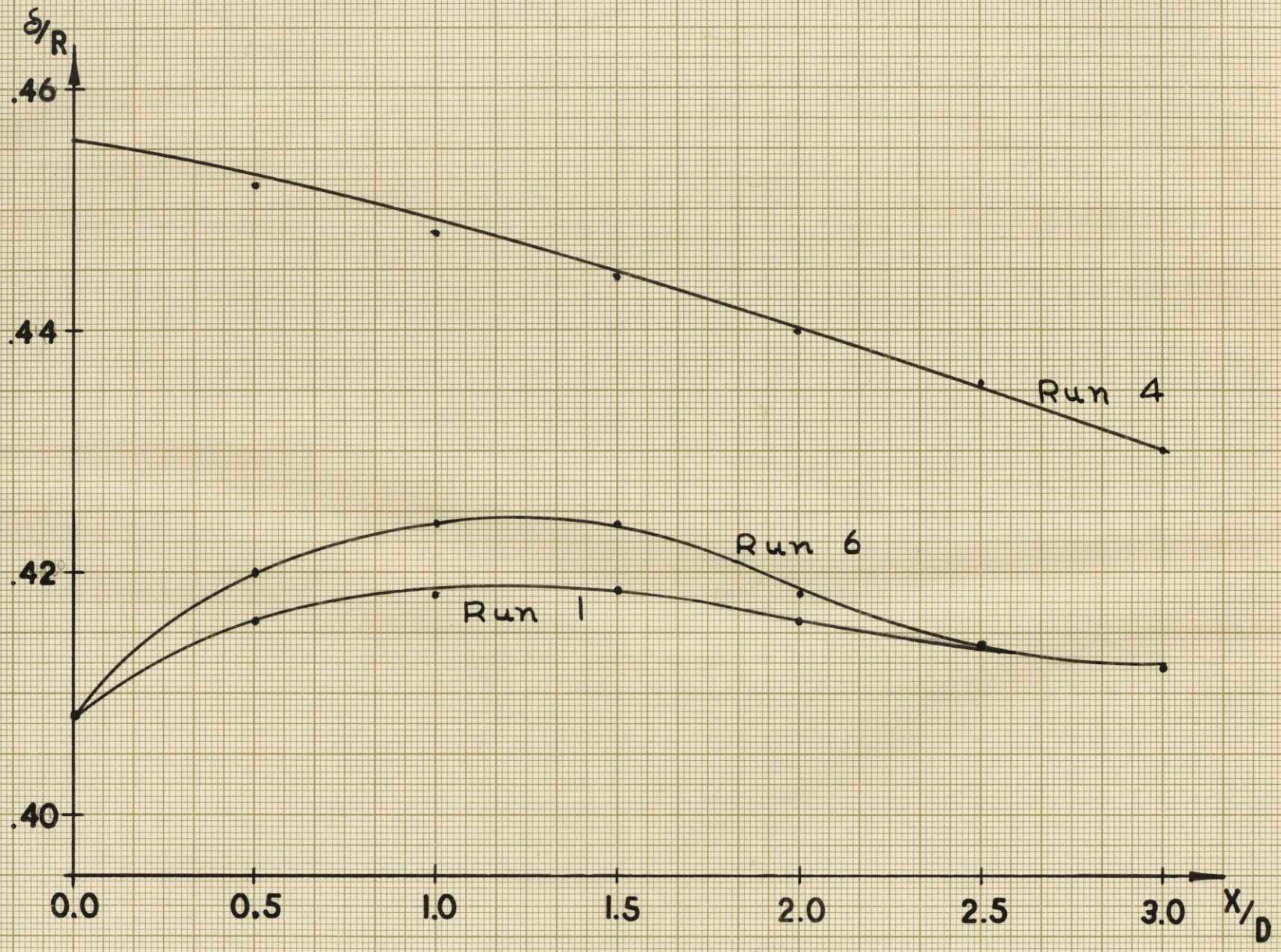

FIGURE 11
BOUNDARY LAYER GROWTH. (FLAT PLATE)

REFERENCES

Gouse, S. William, Jr. "Experimental Investigation of the effects of a Diffustion Field on a Laminar Boundary Layer in Supersonic Flow," M.I.T., Sc.D. Thesis, 1957

Keenan, J. H. and Kaye, J. Gas Tables, (John Wiley & Sons, Inc.), 1948

Prause, R. H., " An Experimental Investigation on the Effects of the Back Pressure on the Pressure Distribution for Compressible Laminar Flow in a Choked-Flow Tube", M.I.T., B.S. Thesis 1960

Rivas, M. A., Jr. and Shapiro, A. H., "On the Theory of Discharge Coefficients for Rounded-Entrance Flowmeters and Venturis". ASME paper No. 54-A-98, 1954

Shapiro, A. H., "The Dynamics and Thermodynamics of Compressible Fluid Flow", Volume I, (New York, Ronald Press Co.), 1953

Thwaites, B., "Approximate Calculation of the Laminar Boundary Layer", The Aero. Quart, I, 245-280, (1949)

Toong, Tan-Yi and Shapiro, A. H., "Theoretical Investigation of the Frictional Effects for Laminar Compressible Flow in a Tube Entry."

A.S.M.E., Flow measurement, (Part 5, Instruments and Apparatus); Supplement to A.S.M.E. Power Test Codes; A.S.M.E., New York, February, 1959

A P P E N D I C E S

Appendix I - DATA TABULATION

Run No. 1

P_o = 1.540 psia

$T_o = 80^oF$

P_b = 0.568 psia

$T_R = 80^oF$

P_{b/P_o} = 0.319

P_{e/P_o} = 0.398

$x/_D$	P(psia)	$P/_{P_o}$	M
0.00	0.613	0.398	1.23
0.50	0.691	0.450	1.13
1.00	0.747	0.488	1.07
1.50	0.788	0.515	1.02
2.00	0.816	0.534	0.99
2.50	0.844	0.552	0.96
3.00	0.854	0.557	0.95

Run No. 2

P_o = 2.20 psia

T_o = 81°F

P_b = 1.370 psia

T_R = 80°F

P_{b/P_o} = 0.678

P_{e/P_o} = 0.678

x/D	P(psia)	P/P_o	M
0.00	1.376	0.678	0.770
0.50	1.390	0.687	0.750
1.00	1.4000	0.695	0.740
1.50	1.410	0.700	0.730
2.00	1.418	0.706	0.722
2.50	1.423	0.710	0.718
3.00	1.432	0.718	0.709

Run No. 3

P_o = 1.950 psia

T_o = 74°F

P_b = 1.209 psia

T_R = 73°F

P_{b/P_o} = 0.620

P_{e/P_o} = 0.620

$x/_D$	P(psia)	$P/_{P_o}$	M
0.00	1.209	0.620	0.854
0.50	1.220	0.626	0.845
1.00	1.238	0.635	0.831
1.50	1.250	0.644	0.821
2.00	1.270	0.653	0.803
2.50	1.282	0.660	0.793
3.00	1.300	0.668	0.781

Run No. 4

P_o = 1.887 psia

T_o = 78°F

P = 1.075 psia

T_R = 77.3°F

P_{b/P_o} = 0.569

P_{e/P_o} = 0.569

$x/_D$	P(psia)	$P/_{P_o}$	M
0.00	1.075	0.569	0.935
0.50	1.092	0.580	0.916
1.00	1.120	0.595	0.893
1.50	1.138	0.605	0.880
2.00	1.150	0.614	0.865
2.50	1.173	0.625	0.846
3.00	1.192	0.637	0.829

Run No. 5

P_o = 1.840 psia

P_b = 0.900 psia

P_{b/P_o} = 0.490

T_o = 77.5°F

T_R = 76.3°F

P_{e/P_o} = 0.490

$x/_D$	P(psia)	$P/_{P_o}$	M
0.00	0.900	0.490	1.062
0.50	0.930	0.505	1.038
1.00	0.970	0.527	1.001
1.50	1.003	0.545	0.972
2.00	1.030	0.561	0.950
2.50	1.059	0.575	0.925
3.00	1.082	0.588	0.905

Run No. 6

P_o = 1.815 psia

T_o = 75°F

P_b = 0.730 psia

T_R = 76°F

P_{b/P_o} = 0.402

P_{e/P_o} = 0.406

$x/_D$	P(psia)	$P/_{P_o}$	M
0.00	0.740	0.406	1.210
0.50	0.850	0.468	1.100
1.00	0.912	0.505	1.036
1.50	0.955	0.526	1.004
2.00	0.985	0.544	0.972
2.50	1.016	0.560	0.950
3.00	1.045	0.575	0.925

Run No. 7

P_o = 1.800 psia

T_o = 79.5°F

P_b = 0.565

T_R = 78.7°F

P_{b/P_o} = 0.314

P_{e/P_o} = 0.400

$x/_D$	P(psia)	$P/_{P_o}$	M
0.00	0.725	0.400	1.223
0.50	0.815	0.452	1.132
1.00	0.886	0.492	1.060
1.50	0.929	0.515	1.019
2.00	0.976	0.543	0.975
2.50	0.990	0.552	0.961
3.00	1.020	0.570	0.932

Appendix II

PRESSURE CONVERSION FACTORS FOR MERCURY AND NARCOIL 40

Gouse, S. William, in his Sc.D. thesis gives the following pressure conversion factors and information:

1. - Pressure Conversion Factors for Mercury.

Temperature $^{o}F.$	Conversion Factor Psi/cm.Hg
70	0.192635
71	0.192616
72	0.192596
73	0.192577
74	0.192557
75	0.192538
76	0.192518
77	0.192499
78	0.192480
79	0.192461
80	0.192442
81	0.192422
82	0.192403
83	0.192383
84	0.192364
85	0.192344
86	0.192325
87	0.192306

2. - Pressure Conversion Factors for Narcoil 40.-

The following conversion factors were used to convert the readings from the manometers to psia. Narcoil 40 is a vacuum diffusion pump oil manufactured by the National Research Corporation. It has a low vapor pressure of 10^{-7} mm.Hg at 77°F and relatively low viscocity, which makes it suitable for use in manometers.

Temperature °F.	Conversion Factor psi/cm.N-40
70	0.013765
71	0.013759
72	0.013754
73	0.013747
74	0.013741
75	0.013735
76	0.013729
77	0.013724
78	0.013718
79	0.013712
80	0.013705
81	0.013700
82	0.013694
83	0.013688
84	0.013682
85	0.013677
86	0.013671
87	0.013666
88	0.013661
89	0.013656